http://resolver.tudelft.nl/uuid:3c28e1fc-8b41-49eb-be8c-0c744604ac25
Primary Topic: Coastal sediment transport (subaqueous and aeolian)
Secondary Topic: Nature-based solutions

FACTORS REGULATING SEDIMENT FLUXES OVER AN ENGINEERED FOREDUNE AND ADJACENT DUNE SLACK

J.J. Oude Vrielink[1,2,3], M.A. Eleveld[2], B. van Westen[2], F. Galiforni-Silva[1,4], and K.M. Wijnberg[1]

[1]Department of Water Engineering and Management, University of Twente, Box 217, 7500 AE, Enschede, the Netherlands. k.m.wijnberg@utwente.nl.

[2]Deltares, Box 177, 2600 MH, Delft, the Netherlands. marieke.eleveld@deltares.nl, bart.vanwesten@deltares.nl.

[3]Currently at Arcadis, Box 220, 3800 AE, Amersfoort, the Netherlands. job.oudevrielink@arcadis.com.

[4]Currently at Coastal Geology and Sedimentology, Department of Geosciences, Christian-Albrechts-Universität zu Kiel, Otto-Hahn-Platz 1, 24118 Kiel, Germany. filipe.galiforni@ifg.uni-kiel.de.

Abstract

This study aims to identify and understand the annual scale sediment transport patterns in a fully engineered dune-dune slack system that was created from seabed sediments for grey dune and moist dune slack habitat creation at the Delfland coast (the Netherlands). The annual morphological development was analysed using LiDAR elevation data. Daily aeolian sediment transport was simulated across the foredune and in the adjacent dune slack, using the numerical aeolian sediment transport model AeoLiS. All simulated transport events were combined to reveal how aeolian sediment transport behaves on an annual scale. Planting two continuous strips of marram grass along the top of the foredune induced rapid growth of the foredune, while limiting sediment supply to the dune slack. The armouring layer of shells that formed at the surface of the engineered topography, functioned as a supply-limiting factor and restricted the sediment entrainment and deflation of the dune slack. Therefore, the formation of a moist dune slack habitat may take longer for this engineered case than in a natural case with similar boundary conditions.

Keywords: Aeolian sediment transport, AeoLiS, engineered dunes, nature-based solutions, foredune, dune slack

1. Introduction

Engineered coasts are increasingly being designed with sediments and vegetation rather than concrete and rock. For sandy shores, this occasionally goes beyond standard practice of beach nourishments, as complete dunes and dune slacks are being created (e.g. Hondsbossche Dunes and Spanjaards Duin, the Netherlands, and Long Beach Island New Jersey, USA). The construction of such engineered dune and dune slack systems can serve the purpose of coastal protection, but also of habitat restoration or compensation for losses of such habitats elsewhere along the coast.

Vegetation in coastal environments is exposed to abrasion by moving grains of sand and salt spray. Where sand fluxes diminish, grey dune habitats with herbs and mosses can develop. Aeolian activity can also deflate the bed of the (secondary) dune slack until the moisture conditions and distance to the groundwater table are suitable for moist dune slack habitat development. Primary dune slacks may be formed when a developing sandy ridge cuts off a portion of beach.

Oude Vrielink, J.J., Eleveld, M.A., van Westen, B., Galiforni-Silva, F., Wijnberg, K.M. (2021). Factors regulating sediment fluxes over an engineered foredune and adjacent dune slack. Proceedings Coastal Dynamics 2021, Delft 28-June-2021 – 02-July-2021. Delft University of Technology, https://doi.org/10.4233/uuid:d44bc4b4-e4b5-4a96-a316-8553c81faba9

These slacks are often long and narrow, run parallel to the shore with an open-end retaining a connection to the sea (Houston, 2008).

So far, coastal dune studies have mainly focussed on natural dunes (e.g. Delgado-Fernandez and Davidson-Arnott 2011; Hesp et al. 2013). Natural dunes are formed by sand that is supplied and sorted by the wind and trapped in a clumpy vegetation cover that has developed naturally in interaction with sediment dynamics (e.g. van der Wal 1998; Reijers et al. 2019). In several aspects, engineered dune systems differ profoundly from these natural systems, as they consist of dredged seabed material that has not been subject to nearshore and aeolian sorting processes and may contain a large amount of shells and shell fragments. In addition, engineered dunes may be planted in regularly spaced patterns. It is yet unclear to what extent the less well-sorted sediment, the applied planting schemes, and the morphologic design affect the aeolian transport patterns emerging at a meso-scale (year) as a cumulative effect from many micro-scale (hourly) transport events.

The paper aims to identify and understand annual (meso-scale) sediment transport patterns that occurred in Spanjaards Duin, an engineered dune-dune slack system at the Dutch coast (Figure 1A). Meso-scale morphological monitoring data are combined with a small-scale process-based model to simulate one year of aeolian sediment transport over the foredune and in the dune slack in order to understand how annual aeolian sediment transport patterns emerge from gross, micro-scale processes.

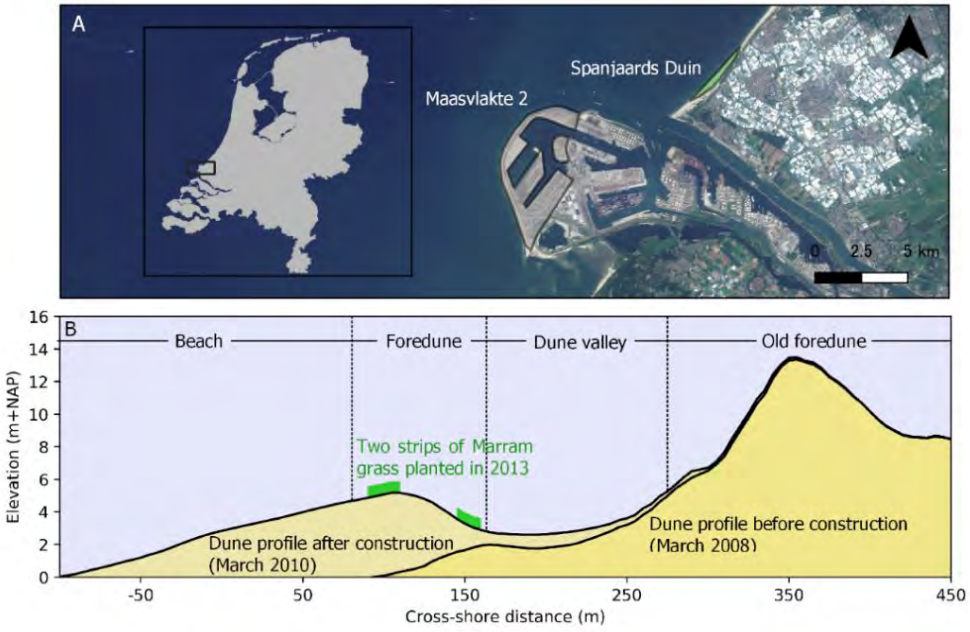

Figure 1. (A) location of the Spanjaards Duin study area (indicated by the green polygon) and (B) cross-shore profile of Spanjaards Duin before and after construction.

2. Study area

Spanjaards Duin, is an artificially created foredune and dune slack area of 0.35 km^2 (35 ha), constructed end 2008 - beginning 2009 as an expansion of the Delfland Coast, the Netherlands (Figure 1A). Spanjaards Duin was created as a compensation measure for the expected increase in nitrogen deposition due to the expansion of the Rotterdam harbour (Maasvlakte 2). Eutrophication

by atmospheric nitrogen deposition stimulates grass encroachment, which outcompetes valuable pioneer vegetation in grey dunes and moist dune slacks. With Spanjaards Duin, a blank canvas for pioneer species was created from marine sands dredged from the North Sea.

Surface (top 10 cm) grain sizes are mainly in the range of 210-420 μm (Veel 2019). A new foredune with a crest at 5 m + NAP (the Dutch reference level, at about mean sea level) was constructed in front of the old foredune (Figure 1B). In between, a low-lying dune slack was created at 2.5 m + NAP. The mean tidal range in the area is 1.75 m. The elongated design showed some similarity to primary dune slack morphology, but without connection to the sea, leaves wind as the main natural sediment transport agent. The coastline is oriented 40° clockwise from north, and the wind often blows from southwesterly directions, as highly shore oblique winds.

In 2013, two strips of European marram grass (*Ammophila arenaria*) were planted on the new foredune to abate transport of sand from the beach into the area designated for dune slack development, whilst deflation could continue to shape the dune slack (van der Meulen et al., 2014).

3. Material and methods

3.1. Meso-scale analysis of monitoring data

Morphological development was studied over the period 2010-2019 using annual elevation (bed level) from airborne LiDAR monitoring data from Rijkswaterstaat. The raster with a grid cell resolution of 5 m had already been filtered for outliers, vegetation and vertical objects, and the error of a single point (described as a RMSE) was 10 to 15 cm (de Graaf et al. 2003). For each year, a mean cross-shore elevation profile was extracted from a raster of 36 longshore cells spanning 180 m.

Hourly mean wind speed with an accuracy of 0.1 m/s, and mean wind direction (in bins of 10 degrees) were obtained from the measurement station Hoek van Holland (lat 51.990° N, lon 4.122° E, 1.3 km south of the centre of the study site) for the period 2010-2019 (KNMI, 2020). The March 2010 - March 2019 study period is characterised by a mean observed hourly wind speed of 7 m/s and a maximum of 22 m/s, higher winds velocities blowing from the sea, and most high wind events from the southwest.

3.2. Micro-scale modelling

Aeolian sediment transport was simulated with the numerical aeolian sediment transport model AeoLiS (Hoonhout and de Vries 2016). AeoLiS is a process-based model that calculates multi-fractional aeolian sediment transport for each sediment fraction separately and includes supply-limiting conditions such as soil moisture. The calculation of the equilibrium aeolian sediment transport concentration is based on the transport formula of Bagnold (1937):

$$q_{sat} = C_b * \sqrt{\frac{d}{D}} * \frac{\rho}{g} * u_*^3 \quad (1)$$

Where the equilibrium or saturated sediment transport rate q_{sat} $[kg/m\,s]$ represents the sediment transport capacity. C_b [-] = an empirical constant related to the sediment type , d [m] = the grain size with respect to a reference grain size D [m], ρ [kg/m^3] = the air density, g [m/s^2] = the gravity constant and u_* $[m/s]$ = the shear velocity. This equation is slightly modified by converting the shear velocity into wind velocity above height z [m] (using the Prandtl-von Kármán equation), including the effect of a velocity threshold above which sand transport occurs u_{th} $[m/s]$, and dividing by the wind velocity u_z to obtain a mass per unit area (or ′concentration in a compressed cube′), c_{sat}:

$$c_{sat} = \alpha * C_b * \sqrt{\frac{d}{D}} * \frac{\rho}{g} * \frac{(u_z - u_{th})^3}{u_z} \quad (2)$$

Saturated transport rates calculated with Equation 1 are often not reached because of supply limiting factors and spatial variability in sediment transport capacity. Therefore, AeoLiS uses an advection equation from which the instantaneous sediment concentration is calculated and is maximized by the available sediment in de bed m [kg/m^2]:

$$\frac{\partial c}{\partial t} + u_z * \frac{\partial c}{\partial x} = \min\left(\frac{\partial m}{\partial t}, \frac{c_{sat} - c}{T}\right) \quad (3)$$

Where c $[kg/m^2]$ represents the instantaneous sediment concentration, t $[s]$ and x $[m]$ denote time and space and c_{sat} $[kg/m^3]$ the saturated sediment concentration calculated from Equation 1. T $[s]$ represents an adaptation timescale of order 1 s (Hoonhout and de Vries 2016).

AeoLiS incorporates vegetation by reducing the shear stress locally where vegetation occurs with a shear stress partitioning approach defined by Raupach (1993) as:

$$\tau_s = \frac{1}{1 + \Gamma * \rho_{veg}} \quad (4)$$

Where τ_s $[N/m^2]$ represents the surface shear stress, Γ [-] = a roughness factor incorporating the effectiveness of shear stress reduction by vegetation and ρ_{veg} [-] = the vegetation density.

3.2.1 Setup

One year (Mar 2014 - Mar 2015) of aeolian sediment transport was simulated in hindcast for an area in Spanjaards Duin containing beach, foredune and a part of the dune slack. The area just south of the Pavilion, centre at 52.000° N, 4.127° E, covers 180 m longshore and 225 m cross-shore with a grid cell resolution of 1 m). Two vegetation strips were implemented in the model using photos obtained by UAV for the location. Vegetation was assumed to cope with increasing bed levels, a constant value in space and time was assumed for vegetation density inside the vegetation strips (ρ_veg = 0.1), and lateral expansion and growth were not included in the model (see Appendix 1 overview of simulation and model parameters).

The simulated waterline functions as an offshore boundary. Inundation of grid cells near the shoreline was calculated based on tidal elevation data from monitoring station at Hoek van Holland (51.978° N, 4.120° E, 2.78 km south of the centre of the study site, Rijkswaterstaat, 2020) and significant wave heights from a permanent wave buoy, Eurogeul E13 (51.999° N, 3.276° E, 58.59 km west of the centre of the study site, Rijkswaterstaat, 2020). Wind forcing was imposed using the monitored wind climate in Hoek van Holland. At the landward boundary sediment transport is zero, meaning that sediment transport from the hinterland is not possible. The lateral boundaries perpendicular to the coastline are provided with circular boundary conditions; the sediment influx at one boundary results in outflux at the next boundary and vice versa.

Five sediment grain size fractions were selected from the measured grain size distribution of August 2017 (Veel, 2019). One extra sediment fraction was added to represent the fraction of shells in the bed. This largest grain size was based on the nominal diameter (d_{n50} $[m]$) calculated from the average weight of 30 shells from the dune slack of Spanjaards Duin (collected on 12 March 2020). It was assumed that 10% of the soil mass contained shells.

The model was calibrated by adjusting the vegetation density and validated by comparing the simulated mean cross-shore elevation profile after 1 year of simulation with the mean bed level profile of March 2015 extracted from monitoring data. The resulting settings (see Appendix 1) were subsequently used to make the model runs.

4. Results

4.1. Observed meso-scale bed level changes

Initially, the development of the constructed foredune and dune slack area was left to naturally occurring dynamics (Figure 2, period March 2010 – March 2013). After the planting of two vegetation strips of marram grass in 2013, the sand accumulated locally at a mean rate of 0.4 m/year in the sea side vegetation strip and 0.2 m/year in the dune slack side vegetation strip. Hardly any accumulation occurred in between the vegetation strips. The dune slack area showed an erosive trend between March 2010 and March 2018. The 0.5 m lower elevation of the dune slack in March 2019 was the result of landscaping (Veel 2019).

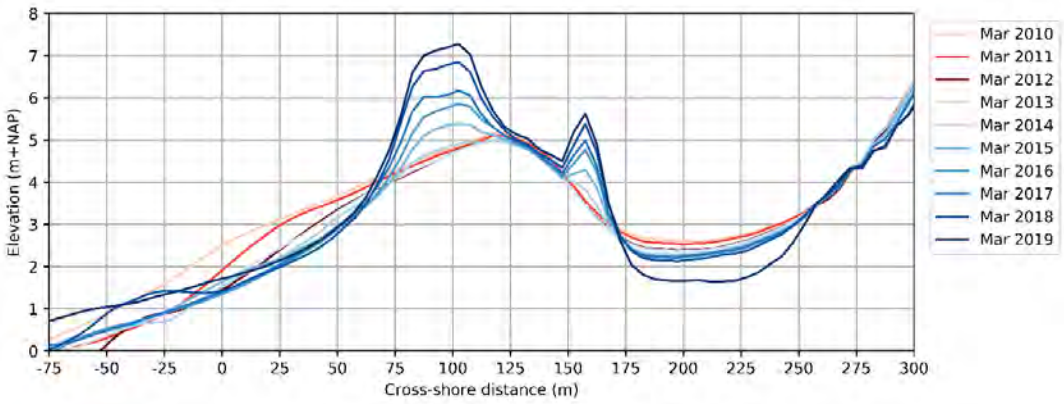

Figure 2. Mean monitored elevation profiles for the period March 2010-March 2019 with pre and post marram grass planting profiles in red and blue respectively.

4.2. Validation of micro-scale model

Figure 3 shows simulated bed level development on a monthly interval for 1 March 2014 to 1 March 2015. An increase in elevation is observed at an average rate of 0.7 m/year inside the sea side vegetation strip and 1.1 m/year in the dune slack side vegetation strip. The latter accumulation rate is strongly overestimated by 0.8 m/year. In the area between the vegetation strips, an erosive trend is simulated but not observed in reality (discrepancy of 0.2 m/year). Erosion of the dune slack is limited. The settings used to produce this cross-shore graph were used to study transport from all directions.

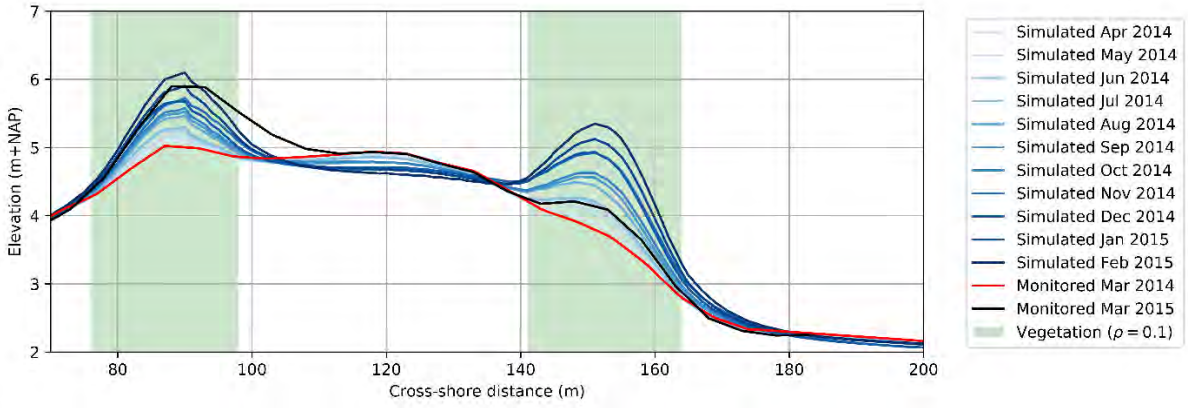

Figure 3. Simulated mean monthly foredune profiles in the period Mar 2014-Mar 2015.

4.3. Micro-scale simulation of surface composition

The simulated multi-fraction grain size distribution in the top (5 cm) layer changes due to aeolian sediment transport in the first 15 days of simulation (Figure 4). On the bare part of the foredune and in the dune slack, the sediment grain size distribution (Figures 4A and B) and mass (Figures 4D and F) tend towards the larger sediment fractions, including the fraction representing shells (d=6 mm). Inside the vegetation strips deposition of fine sediment results in a changing sediment grain size distribution dominated by smaller particles.

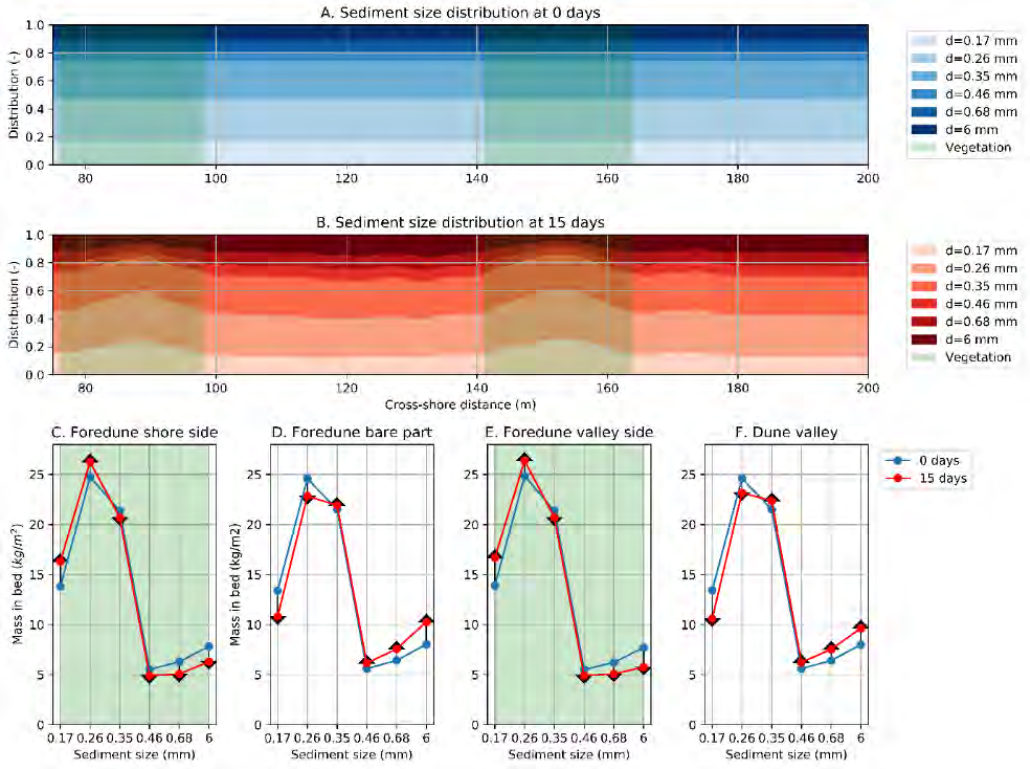

Figure 4. Simulated sediment grain size distribution in the top (5 cm) layer showing (A) the initial sediment distribution, and (B) the distribution after 15 days. Shells correspond with d=6 mm. The changing mass of the grain size fractions in the bed surface layer is shown for the vegetated parts (C and E) and the bare parts (D and F). Direction of change as black arrows.

4.4. Simulated daily aeolian sediment transport

Figure 5 shows the relation between the wind speed (distance from the origin), wind direction (angle in the plot) and the simulated daily aeolian sediment transport rates (colour) for different parts on the foredune (A, B and C) and in the dune slack (C). The threshold wind velocity for aeolian sediment transport differs per grain size, but the model results showed that substantial transport rates occur above 10 m/s. Aeolian sediment transport rates decrease when moving from the foredune to the dune slack, except during the 20 m/s storm event from the northwest (21 October 2014, after 235 days in the simulation) (compare Figures 5A-D).

4.5. Simulated net annual aeolian sediment transport

A map of simulated overall net aeolian sediment transport on an annual scale from summed individual transport events, can be understood by examining the relative importance of (high

magnitude) wind events from different directions (Figure 5). It confirms the importance of the longshore component, particularly along the dune slack, and shows increase near foredune crest and deflection of the annual aeolian sediment transport along the cross-shore profile (Figure 6B).

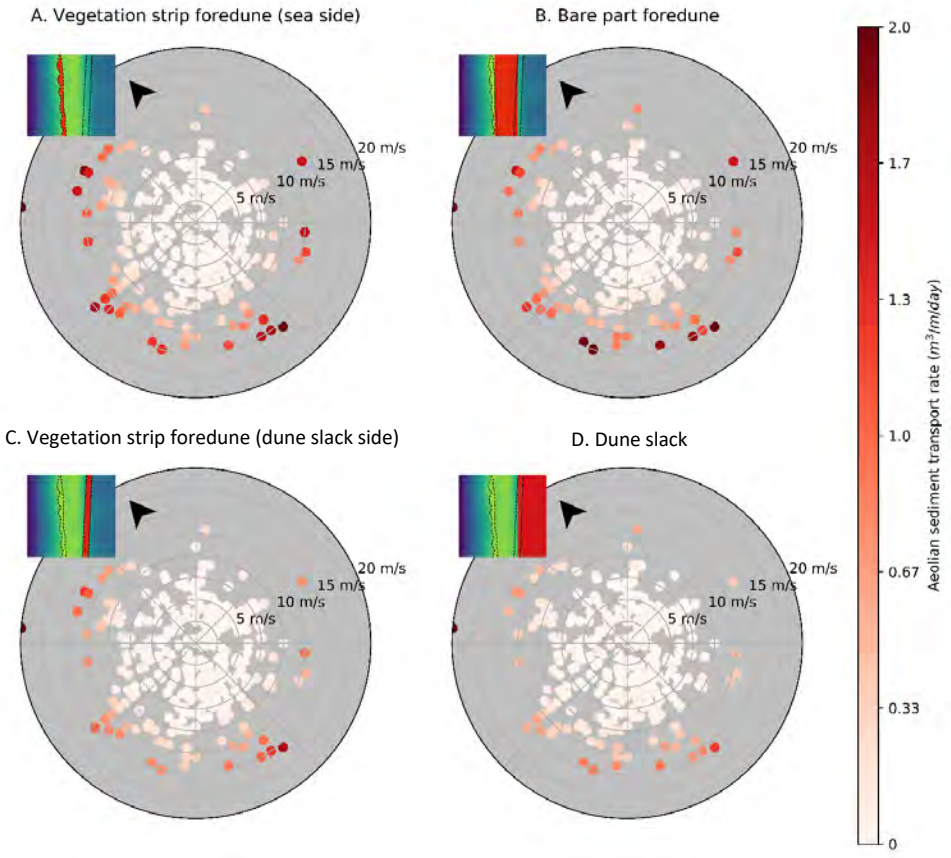

Figure 5. Polar plots showing the relation between wind speed (distance from the origin), wind direction (angle in the plot) and the area averaged simulated aeolian sediment transport rates (colours) for daily events on different parts of the foredune (A, B and C) and dune slack (D). Top left maps indicate the analysed areas in red.

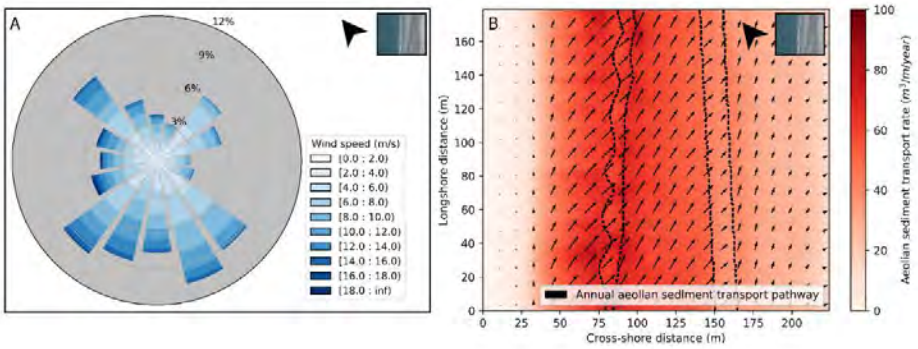

Figure 6. (A) Wind climate of simulated period and (B) map of simulated annual aeolian sediment transport field including magnitude (colour) and direction (arrow). Arrow size indicates the transport magnitude. The wind data and the model grid are rotated 40° counter clockwise so that the model grid is orientated perpendicular to the dune foot.

5. Discussion

The transport limiting impact of the groundwater table (0.8 - 1.80 m above + NAP (Veel 2019) was not taken into account in the simulations, whilst capillary fringe can impact soil moisture content and aeolian transport from the beach and locally in the valleys (see Figure 5). The model does show that many low magnitude wind events do not result in aeolian sediment transport since the threshold shear velocity for saltation is not reached (Figure 6; Bagnold 1937; Delgado-Fernandez 2011). Wind events above the assumed threshold for to aeolian sediment transport (Figure 6) are often accompanied by limiting factors, such as precipitation (Delgado-Fernandez and Davidson-Arnott 2011). We did not take precipitation into account, which can contribute to our overestimation of sediment entrainment.

In the bare dune slack, and locally between the vegetation strips on the foredune, sediment sorting and the emergence of non-erodible layers resulted in a stabilized bed surface layer dominated by shell fragments (Figures 5D, F). This is distinctive for nourished material and limits the aeolian activity in engineered beach environments (van der Wal, 1998; Hoonhout and de Vries, 2017). Erosion between the vegetation strips is overestimated. No spin-up time was used in the simulation. Therefore, the initial stage of sediment sorting, when the sediment transport rates are relatively high, is included in the model, while in reality the bed was probably already stabilized. Furthermore, the shell fragments covering the surface were parameterized as round sediment particles which may be entrained more easily than shell-shaped particles of similar weight.

The influx of sand from the beach and bare areas on the foredune into the valley, the initial construction height of the dune slack and the redistribution of sand available for transport in the dune slack, as well as the slow-down of the deflation because of the shell pavement caused the stabilized engineered dune slack to develop differently from a natural case in which dune slacks develop gradually by deflation of the surface until the local water table has been reached after which colonization and establishment of moist dune slack vegetation occur (Houston 2008). For Spanjaards Duin this has been stimulated by excavation of five gently sloping ponds and depositing in total 40 thousand m^3 of sand on the shoreline in January 2019 (Figure 3; and Veel 2019), because the dune area should accommodate extensive areas of high-quality grey dune and moist dune slack vegetation, within a set time frame of 25 years.

The accumulation inside the vegetation (Figures 3 and 5) is caused by a decrease in flow velocity inside the vegetation canopy for moderate wind events (just above threshold) caused by the increased roughness (Hesp et al. 2013), and is responsible for the decrease of aeolian sediment transport rates across the foredune (Figures 6 and 7). After the planting of two vegetation strips in 2013, monitoring data showed the foredune to adapt fast and develop as a foredune in which the vegetation growth was able to keep up with the accumulation rates (Figure 3) within ranges for naturally developed dunes with European marram grass (Reijers et al. 2019). An additional explanation for overestimation of accumulation rates in the dune slack side vegetation strip (Figure 5) could be an underestimation of the sediment capturing capacity of the first row of vegetation.

Generally, the initial construction height and the uninterrupted vegetation strips make the situation different from a natural case in which embryonal foredunes are gradually formed consisting of patches of marram grass where in between aeolian sediment transport pathways facilitate the supply of sediment into the dune slack.

6. Conclusion

The high shell content of the engineered foredune and dune slack, which is much higher than would normally occur in a naturally formed dune-dune slack system, caused surface armouring and hence lowered rates of sediment entrainment over the bare areas, and stabilized the bed level in potential zones of erosion. Due to this higher transport velocity threshold, the meso-scale sand transport flux is controlled by higher wind speeds than in a natural case where such armouring does not occur. The surface armouring in the engineered dune slack slows down the deflation to the groundwater level and implies that the formation of secondary dune slacks in engineered environments may take longer.

The planted continuous marram grass strips showed to be an effective sand trap to accelerate foredune growth, and reduced aeolian sediment transport rates into the adjacent dune slack. The fact that no openings are present in between individual plants implies that in this engineered case the aeolian sediment transport patterns across the foredune are different compared to a natural case in the sense that less sediment transport pathways can be created across the foredune.

Acknowledgements

This research was conducted within the frame of SPA PMR MEP duinen 2018-2020 project, which was funded by Rijkswaterstaat-WVL. We further want to thank Lisa Meijer for providing her AeoLiS model version, and the Spanjaards Duin project team for their support in analyzing the monitoring data and providing relevant feedback.

Data and code availability

Monitoring data is available on request through https://repos.deltares.nl/repos/MEPDuinen/trunk/Spanjaards_Duin (for bed level elevation and sediment surface composition in Spanjaards Duin). The AeoLiS model is available from https://github.com/openearth/aeolis-python, the version that was tested here from https://github.com/lisameijer/aeolis-python.

Appendix 1 Simulation and model parameters

Symbol	Parameter	Value(s)	Unit
n_x, n_y	Cells in x- and y-direction	224, 179	-, -
Δx, Δy	Cell size in x- and y-direction	1	m, m
Δt	Time step	1800	s
t_{stop}	Simulation length	31536000 (1 year)	s
$n_{fraction}$	Number of sediment fractions	6	-
n_{layers}	Number of layers	3	-
d_{layer}	Layer thickness	0.05	m
$d_{sediment}$	Sediment sizes	0.17, 0.26, 0.35, 0.46, 0.68, 6	mm
$dist_{sediment}$	Sediment grain size distribution	0.17, 0.31, 0.27, 0.08, 0.1	-
ρ_{air}	Air density	1.225	kg/m^3
$\rho_{sediment}$	Sediment density	2650	kg/m^3
T_{dry}	Adaptation time scale for soil drying	7200	s
T	Adaptation time scale for advection equation	1.0	s
β	Ratio between drag coefficient of roughness elements and bare surface	30	-

bi	Bed interaction factor	0	-
$accfac$	Numerical acceleration factor	1	-
V_{veg}	Characteristic vegetation growth	0	$m/year$
V_{lat}	Lateral vegetation growth	0	$m/year$
γ_{veg}	Constant on influence of sediment burial	0	-
ρ_{veg}	Vegetation cover	0.1	-

References

Bagnold, R. 1937. The transport of sand by wind. *Geogr. J*, 89 (5), 409-438. doi:10.2307/1786411

de Graaf, H., Oude Elberink, S., Bollweg, A., Brügelmann, R. and Richardson, L. 2003. *Inwinning "droge" JARKUS profielen langs Nederlandse kust*, http://publicaties.minienm.nl/documenten/inwinning-droge-jarkus-profielen-langs-nederlandse-kust-vergelij

Delgado-Fernandez, I. 2011. Meso-scale modelling of aeolian sediment input to coastal dunes. *Geomorphology*, 130, 230–243. doi:10.1016/j.geomorph.2011.04.001

Delgado-Fernandez, I. and Davidson-Arnott, R. 2011. Meso-scale aeolian sediment input to coastal dunes: The nature of aeolian transport events. *Geomorphology*, 126 (1), 217-232. doi:10.1016/j.geomorph.2010.11.005

Hesp, P., Walker, I., Chapman, C., Davidson-Arnott, R., Bauer, B. 2013. Aeolian dynamics over a coastal foredune, Prince Edward Island, Canada. *Earth Surf. Process. Landf.*, 38, 1566-1575. doi:10.1002/esp.3444

Hoonhout, B. and de Vries, S. 2016. A process-based model for aeolian sediment transport and spatiotemporal varying sediment availability. *J. Geophys. Res. Earth. Surf.*, 121 (8), 1555-1575. doi:10.1002/2015JF003692

Hoonhout, B. and de Vries, S. 2017. Aeolian sediment supply at a mega nourishment. *Coast. Eng.*, 123, 11-20. doi:10.1016/j.coastaleng.2017.03.001

Houston J. A. 2008. *Management of Natura 2000 habitats. 2190 Humid dune slacks*, EC, https://ec.europa.eu/environment/nature/natura2000/management/habitats/pdf/2190_Humid_dune_slacks.pdf

KNMI. 2020. *Uurgegevens van het weer in Nederland*, http://projects.knmi.nl/klimatologie/uurgegevens/selectie.cgi.

Raupach, M., Gillette, D. and Leys, J. 1993. The effect of roughness elements on wind erosion threshold. *J Geophys Res Atmos.*, 98 (D2), 3023-3029. doi:10.1029/92JD01922

Reijers, V., Siteur, K., Hoeks, S., van Belzen, J., Borst, A., Heusinkveld, J., Govers, L., Bouma,T., Lamers, L., van de Koppel, J. and van der Heide, T. 2019. A Lévy expansion strategy optimizes early dune building by beach grasses. *Nat. Commun.*, 10 (1). doi:10.1038 /s41467-019-10699-8

Rijkswaterstaat 2020. *Rijkswaterstaat waterinfo*, https://waterinfo.rws.nl.

van der Wal, D. 1998. The impact of the grain-size distribution of nourishment sand on Aeolian sand transport. *J. Coast. Res.*, 14 (2), 620-631.

van der Meulen, F., van der Valk, B., Baars, L., Schoor, E. and van Woerden, H. 2014. Development of new dunes in the Dutch Delta: nature compensation and `building with nature'. *J. Coast. Conserv.*, 18 (5), 505-513. doi:10.1007/s11852-014-0315-2

Veel, P. (ed.) 2019. [With contributions of Arens, S., Beekman, W., Poot, S. and others] *Jaarverslag beheer Spanjaards Duin 2018*, Zuid-Hollands Landschap. https://repos.deltares.nl/repos/MEPDuinen/trunk/Spanjaards_Duin